Article

Journal of Nanoscience and Nanotechnology
Vol. 14, 9614–9618, 2014
www.aspbs.com/jnn

Characteristics of Pulsed Internal Inductively Coupled Plasma for Next Generation Display Processing

Tae Hyung Kim[1], Seung Min Lee[1], Chul Hee Lee[1], Jeong Oun Bae[1], Geun Young Yeom[1,2,*], and Kyong Nam Kim[1,*]

[1] *Department of Advanced Materials Science and Engineering, Sungkyunkwan University, Suwon 440-746, Korea*
[2] *Sungkyun Advanced Institute of Nanotechnology (SAINT), Sungkyunkwan University, Suwon 440-746, Korea*

RF pulsed plasma characteristics of inductively coupled plasma (ICP) sources operated with internal linear type antennas for the next generation display processing were investigated. By applying the rf pulse mode in the ICP source, with decreasing the rf pulse duty percentage, the average electron temperature was decreased and the plasma non-uniformity was improved with decreasing the rf pulse duty percentage. In the case of plasma uniformity, for the same time average rf power of 3 kW to the ICP source, the plasma non-uniformity was improved from 8.4% at 100% of rf duty percentage to 6.4% at 60% of rf duty percentage due to the increased diffusion of the plasma during the pulse-off time. When SiO_2 was etched using CF_4, the etch rate uniformity was also improved due to the improvement of plasma uniformity.

Keywords: Flat Panel Display, Internal Inductively Coupled Plasma/Icp, Pulsed Plasma, CF_4.

1. INTRODUCTION

Plasma processing is one of the key technologies for manufacturing of electronic device such as semiconductor, flat panel displays (FPDs), photovoltaic devices etc.[1–4] Especially, because the critical dimension of the most of the electronic devices shrink to nanometer scale sizes and the devices are highly integrated, the necessity for more precise control of the plasma variables required for the fabrication of these devices is also increased.

Recently, in the case of semiconductor industry, to meet the critical specification of tens of nanometer-size semiconductor device fabrication, various plasma techniques such as rf pulsing have been introduced and verified the control of plasma variables such as electron energy distribution, therefore, the control of gas dissociation characteristics in the plasma. In addition, by using the pulsed plasmas, the decrease of charging on the wafer surface during the pulse-off time during the pulsing, the improvement of plasma uniformity over the wafer surface due to the increased diffusion, and improved anisotropic etch profile during the reactive ion etching could be obtained even though the processing rates are decreased due to the existence of pulse-off time during the plasma processing.[5–8]

Similarly, for the next generation display applications such as large area FPDs and flexible displays, the control of plasma variables has become very important as the substrate size is increased to a few meter scale, as the display pixel size is decreased, and as the number of pixel size is increased in addition to the requirement of low temperature and low damage processing.[9,10] Especially, as the displays move to the large area FPDs and flexible displays, the device damage by the plasma exposure and the processing uniformity over the large area substrate have become the important issues for the next generation display processing.[11,12] To overcome some of these problems and to control the plasma variables, various techniques such as the use of multiple short antennas, the use of magnetic field, the use of a multiple helicon plasma source, etc. have been investigated.[13–15] However, for more precise control of the plasma variables and to overcome the problems such as controlling the plasma uniformity, improving the etch selectivity, reducing the electrical damage, etc., rf pulsing techniques used for semiconductor applications may need to be investigated.

In this study, an ICP source composed of four internal-type linear antennas has been studied as the application to next generation displays and the effects of rf pulsing of the ICP antenna on the plasma characteristics were

*Authors to whom correspondence should be addressed.

1533-4880/2014/14/9614/005 doi:10.1166/jnn.2014.10184

investigated. For the pulsed ICP plasma, 13.56 MHz of rf pulsed power supply (SEREN R10001) was connected, and the plasma characteristics such as electron temperature, plasma non-uniformity, and radicals in the plasma were investigated for the continuous wave(CW) mode and the pulsed mode.

2. EXPERIMENTAL DETAILS

The schematic diagram of the internal ICP system used in this study is shown in Figure 1. In the figure, the locations of the emissive probe and the electrostatic probe installed in the chamber used to measure the plasma characteristics are also shown. The processing chamber has a rectangular shape with the size of 2,750 mm × 2,350 mm, and the substrate size was 2,300 mm × 2,000 mm for the applications to large-area FPD processing. The area of plasma source to be installed, however, was 1,000 mm × 2,000 mm, which didn't cover overall area mentioned above because of the limitation such as rf power capacity when the pulse mode was applied. As shown in Figure 1, the double comb-type antenna was connected to a 10 kW of 13.56 MHz rf pulsed power supply (SEREN R10001) through an *L*-type matching network while the other side was connected to ground. The antenna was made of 19 mm-diameter copper tubing to allow for water cooling, and was covered by ceramic tubing for dielectric isolation from the plasma.

All experiments were carried out at 10 mTorr of CF_4 and the rf power was varied from 3 kW to 5 kW. A homemade emissive probe was installed at center of chamber and located at 20 cm below the antenna for the measurement of instant/time-average plasma characteristics during the rf pulsing. Using the emissive probe, the instant/time average electron temperature could be calculated from the changes of instant plasma potential and instant floating potential using the equation relating electron temperature, plasma potential, and floating potential as shown below[16]

$$V_p - V_f = \frac{kT_e}{2e} ln\left(\frac{\pi m}{2M}\right) \quad (1)$$

where, V_p and V_f are the plasma potential and the floating potential, respectively, k is the Boltzmann constant, T_e is electron temperature, m is electron mass, and M is the atomic mass. A movable electrostatic probe was used for the plasma uniformity by measuring the ion saturation current by biasing the probe at −30 Volts and by scanning the probe from 0 mmv (edge) to 600 mm (center). An optical emission spectroscope (OES, Andor Inc., model: SR-303i-A) was used to observe the gas dissociation characteristics of CF_4 used in the experiment. For more accurate measurement of dissociated gas ratios from CF_4, Ar actinometry was used by adding 10% of Ar to CF_4 gas and by measuring the ratio of I_F(703 nm)/I_{Ar}(750.1 nm), I_{CF2}(275.4 nm)/I_{Ar}(750.1 nm), etc.

3. RESULTS AND DISCUSSION

Figure 2 shows the instant plasma potential (V_p) and the instant floating potential (V_f) measured as a function of operation time using an emissive probe for 5 kW of rf power to the ICP power and 60% rf duty percentage. As the operating gas, 10 mTorr of CF_4 gas was used. The measurement was carried out at the center of the chamber and about 20 cm below the antenna as shown in the inset of Figure 3. As shown in the figure, during the pulse-on time, the V_p was about 13 V while the V_f is about −10 V except for the initial transition period and, during the pulse-off time, the V_p was close to 0 V while V_f is increasing from −10 to near 0 V. In the figure, the instant electron temperature calculated from the instant V_p and the instant V_f is also shown, and, the instant electron temperatures were

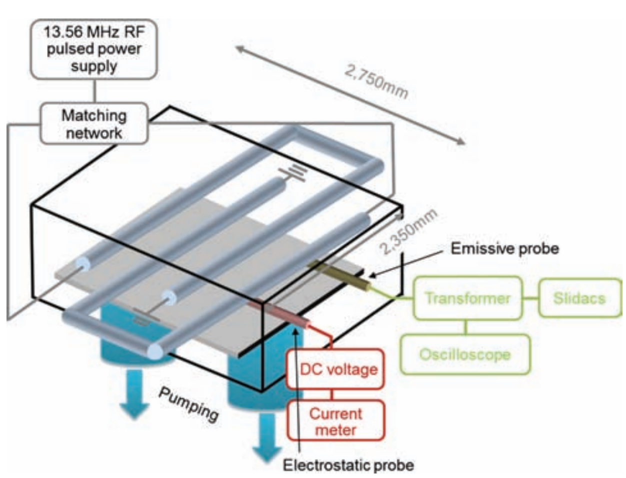

Figure 1. Schematic diagram of an internal-type linear ICP system, a homemade emissive probe and an electrostatic probe used in this experiment.

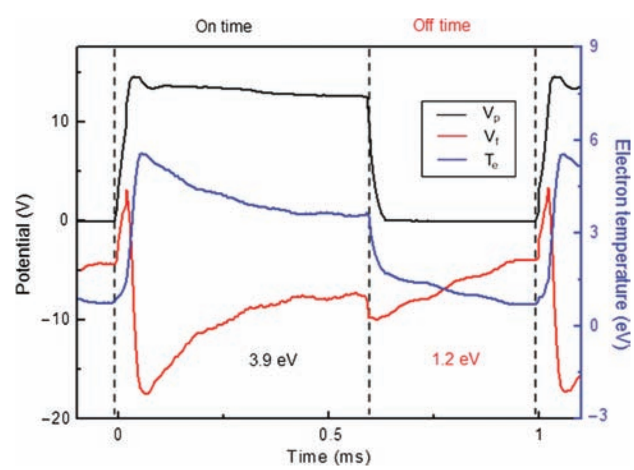

Figure 2. Instant plasma potential (V_p) and the instant floating potential (V_f) measured as a function of operation time using an emissive probe for 5 kW of rf power to the ICP power and 60% rf duty percentage. As the operating gas, 10 mTorr of CF_4 gas was used. The instant electron temperature calculated from the instant V_p and the instant V_f is also shown.

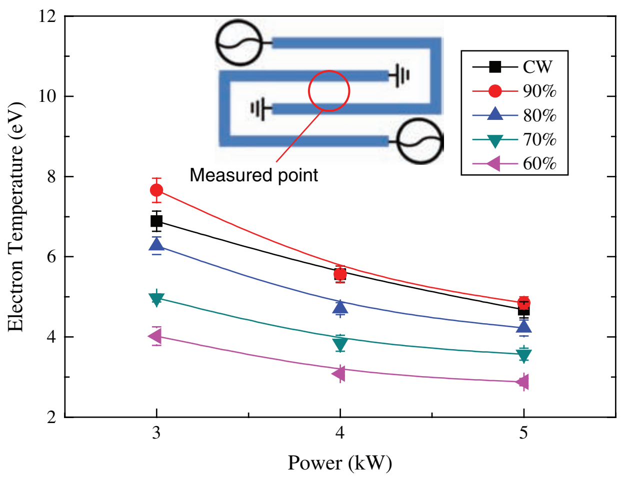

Figure 3. Electron temperature estimated by an emissive probe as a function of pulse condition for CF_4 plasma.

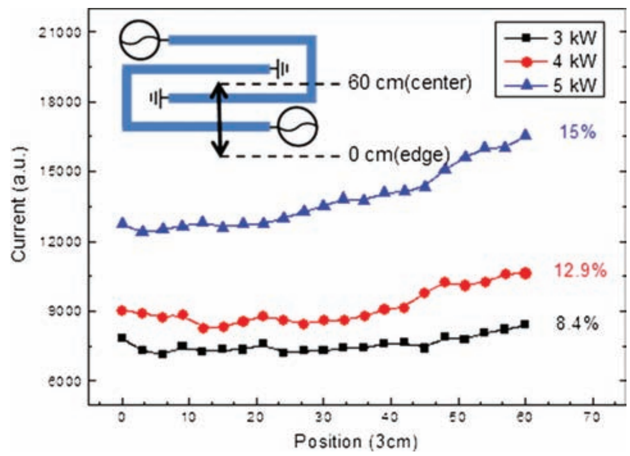

Figure 4. Plasma non-uniformity measured by an electrostatic probe as a function of CW rf power at CF_4 plasma.

about 3.9 eV during the pulse-on time and 1.2 eV during the pulse-off time.

Using the instant electron temperature data obtained for the different rf powers to the ICP source from 3 kW to 5 kW and for the rf duty percentage from CW(100%) to 60%, the average electron temperature was calculated and the results are shown in Figure 3. As shown in the figure, the increase of rf power to the ICP source generally decreased the average electron temperature, for example, during the CW operation, by decreasing from 6.9 eV at 3 kW to 4.7 eV at 5 kW. The decrease of average electron temperature with increasing the rf power to the ICP source is believed to be related to the change of plasma mode from a CCP mode to an ICP mode. At the same rf power to the ICP source, the decrease of rf duty percentage also decreased the average electron temperature, for example, at 5 kW of rf power, by decreasing from 4.7 eV at the CW operation to 2.9 eV at the 60% duty percentage, due to no plasma during the pulse-off time.

Using an electrostatic probe, the plasma uniformity across the internal ICP source antenna was measured as a function of rf power to the ICP source during the CW operation and with 10 mTorr CF_4 and the results are shown in Figure 4. The ion saturation current was measured as an estimation of plasma density and the ion saturation current was measured along the center line of the chamber and from the edge (0 mm) to the center (600 mm) across the antenna line. The measured direction is also shown in the inset of the figure. As shown, the increase of rf power to the ICP source degraded the plasma uniformity in the chamber by increasing the plasma non-uniformity from 8.4 to 15% while increasing the rf power from 3 to 5 kW even though the ion saturation current was increased with the increase of rf power to the ICP source indicating the increased plasma density with the increase of rf power. The decrease of non-uniformity of the plasma in the large area internal ICP system is probably related to the non-uniform power distribution among the four linear antennas, the difficulty in diffusion of plasma along the meter scale distance, etc.[17]

Therefore, to improve the plasma non-uniformity, rf pulsing was applied to the ICP source and the effect of rf pulsing on the plasma uniformity was investigated. Figure 5(a) shows the ion saturation current measured along the center line of the chamber using an electrostatic probe from the edge (0 mm) to the center (600 mm) across the antenna line. The other experimental conditions are the same as those in Figure 4 except for the pulsing from CW(100%) to 60% at 3 kW of rf power. As shown in the figure, the application of rf pulsing and the decrease of rf pulse duty percentage improved the plasma uniformity by showing 8.4% for CW, 6.4% for 80% of rf duty percentage, and 4.9% for 60% of rf pulse duty percentage even though the ion saturation current was decreased with the decrease of rf duty percentage.

The improvement of plasma uniformity by the rf pulsing and with the decrease of pulse duty percentage might be related to the decrease of rf power to the ICP source because the average rf power to the chamber is decreased with the decrease of rf duty percentage. Therefore, the rf power to the ICP source during the rf pulsing was compensated to have the same average rf power to the chamber and the plasma uniformity was measured again. Figure 5(a) also shows the ion saturation current measured along the center line of the chamber (and across the antenna line) for the 5 kW rf power during rf pulsing at 60% duty percentage to have the same average rf power of 3 kW. As shown, even with the compensated rf power of 3 kW, the uniformity was improved to 6.4% (5 kW, 60% duty percentage = average 3 kW) from 8.4% (3 kW CW) while no significant differences in the average ion saturation currents between the compensated power (5 kW 60% duty) and the CW power (3 kW CW) are observed indicating similar plasma densities for both conditions.

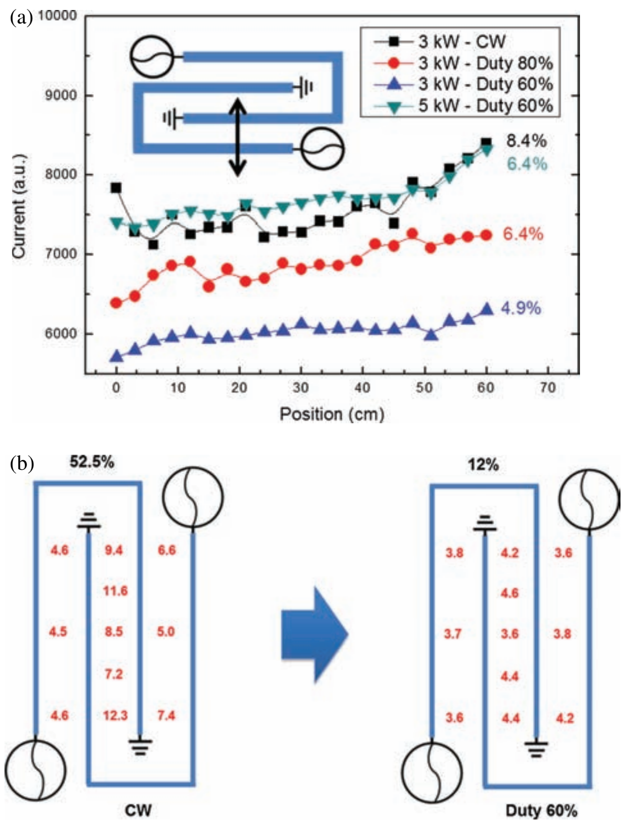

Figure 5. (a) Plasma non-uniformity measured by ion saturation current probe and (b) SiO_2 etch non-uniformity at CW and 60% of rf pulse duty percentage of 3 kW rf power without biasing the substrate. In (a), plasma uniformity measured at 5 kW and 60% duty percentage was also included to compare with 3 kW CW condition as the same average rf power of 3 kW.

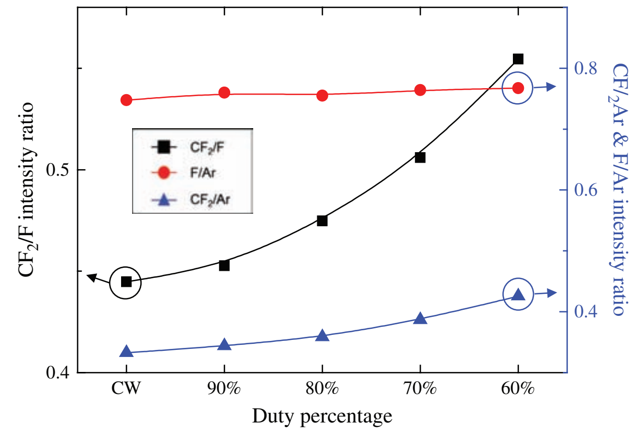

Figure 6. Relative concentrations of $CF_2(I_{CF2}/I_{Ar})$ and $F(I_{CF2}/I_{Ar})$ measured by OES using Ar actinometry. The concentration ratio CF_2/F ratio measured as a function of pulse duty percentage at the gas mixture of an Ar/CF_4 (1:9) was also included.

In fact, the measurement of plasma density shown in Figures 4 and 5(a) is limited to the centerline of the chamber and it may not be representing the plasma uniformity over the large area substrate surface. Also, rather than the plasma uniformity, the etch uniformity on the substrate is more important. Therefore, using SiO_2 wafers, the uniformity of SiO_2 etch rates over the substrate are was measured for the conditions of 3 kW CW rf power and 3 kW 60% rf pulse duty percentage and the results are shown in Figure 5(b). In this experiment, no biasing was applied to the substrate. The measured locations are shown in the figure. As shown in the figure, across the antenna line, the SiO_2 etch rate was higher at the center of the chamber and decreased at the edge of the chamber, therefore, the etch uniformity profile was similar to the plasma uniformity profile shown in Figure 5(a). However, possibly due to the additional non-uniformity of the plasma along the antenna line, the etch non-uniformity measured for the CW condition was as high as 52%. However, by using 60% rf pulse duty percentage, the etch non-uniformity was improved to 12% due to the diffusion of plasma along the chamber during the pulse-off time. Therefore, by using the rf pulsing, the improvement of plasma etch uniformity over a meter scale substrate could be obtained.

The application of rf pulsing changes the electron temperature as shown in Figures 2 and 3, therefore, it can change the gas dissociation characteristics in the plasma. Figure 6 shows the relative concentrations of CF_2 (I_{CF2}/I_{Ar}) and $F(I_{CF2}/I_{Ar})$ measured by OES using Ar actinometry. In fact, for the Ar actinometry, less than 5% Ar is generally used, but due to the low signal intensity of Ar during the pulse operation, we used 10% of Ar added to CF_4. 3 kW of 13.56 MHz rf power was applied to the ICP source while varying the rf pulse duty percentage from CW(100%) to 60%. 10 mTorr of Ar/CF_4 (1:9) was used. Using the OES, intensities of CF_2 radical peak (275.4 nm) known as one of the polymer precursors and F peak (703 nm) used to etch SiO_2 were observed together with Ar peak intensity (750.1 nm).[18–20] As shown in Figure 6, the decrease of rf pulse duty percentage did not change the F concentration (I_F/I_{Ar}) significantly but it increased the CF_2 concentration $((I_{CF2}/I_{Ar})$. Therefore, as shown in the figure, the ratio of CF_2/F was increased with decreasing the pulse duty percentage. The increase of CF_2/F ratio in the plasma can improve the etch selectivity during the etching of SiO_2 by increasing the etch selectivity over the photoresist.

4. CONCLUSION

In this study, the effect of rf pulsing on the plasma characteristics of internal-type ICP sources for the next generation large area processing have been investigated. By applying the rf pulsing and by decreasing the rf pulse duty percentage during the operation of ICP source, the average electron temperature was decreased, and, the dissociation of CF_4 changed to CF_2-rich by showing higher CF_2/F ratio. Also, the plasma non-uniformity improved with decreasing the rf pulse duty percentage by showing 6.4% at 60% rf duty percentage from 8.4% at CW for the same time average rf power of 3 kW to the ICP source. The SiO_2 etch uniformity was also improved by using the rf pulsing due to the improvement plasma uniformity. It is believed that, by using the rf pulsing technique to the ICP source applied to display processing, various advantages such as the improvement of etch selectivity, improved etch uniformity, etc. can be obtained.

Acknowledgments: This work was supported by the Industrial Strategic Technology Development Program (10041681, Development of fundamental technology for 10 nm process semiconductor and 10 G size large area process with high plasma density and VHF condition) and the International Joint Research and Development Program (N009300229, Large area PECVD Equipment development for Flexible low temperature high density film deposition) founded by the Ministry of Knowledge Economy (MKE, Korea)

References and Notes

1. A. J. Holland, M. Barnes, A. Demos, T. Ni, P. Shufflebotham, and W. Yao, *SID Sym. Digest* 27, 526 **(1996)**.
2. F. Heinrich, U. Banzlger, A. Jentzsch, G. Neumann, and C. Huth, *J. Vac. Sci. Technol. B* 14, 2000 **(1996)**.
3. H. Takei, H. Kawamura, Y. Ohta, and R. Gardner, *SID 98 Digest* 29, 1102 **(1998)**.
4. J. Schmitt, M. Elyaakoubi, and L. Sansonnens, *Plasma Sources Sci. Technol.* 11, A206 **(2002)**.
5. S. Samukawa, *Jpn. J. Appl. Phys.* 33, 2133 **(1994)**.
6. I. G. Kim, N. S. Kim, J. S. Park, and D. Y. Park, *Jpn. J. Appl. Phys.* 41, 2380 **(2002)**.
7. H. Ohtake and S. Samukawa, *J. Vac. Sci. Technol. B* 20, 1026 **(2002)**.
8. H. Ohtake, B. Jinnai, Y. Suzuki, S. Soda, T. Shimmura, and S. Samukawa, *J. Vac. Sci. Technol. A* 24, 2172 **(2006)**.
9. J.-S. Na and O.-K. Kwon, *Jpn. J. Appl. Phys.* 53, 03CD02 **(2014)**.
10. G.-J. Lv, W.-X. Zhao, J. Wang, and Q.-H. Wang, *Optik* 125, 1984 **(2014)**.
11. W. Z. Collison, T. Q. Ni, and M. S. Barnes, *J. Vac. Sci. Technol. A* 16, 100 **(1998)**.
12. Y. Wu and M. A. Lieberman, *Plasma Sources Sci. Technol.* 9, 210 **(2000)**.
13. Y. J. Kim, S. H. Han, W. Hwang, and Y. S. Hwang, *Thin Solid Films* 435, 270 **(2003)**.
14. K. Takenka, Y. Setsuhara, K. Nishisaka, and A. Ebe, *Jpn. J. Appl. Phys.* 47, 6900 **(2008)**.
15. T. Meziani, P. Colpo, and F. Rossi, *Plasma Sources Sci. Technol.* 10, 276 **(2001)**.
16. A. Mishara, M. H. Jeon, K. N. Kim, and G. Y. Yeom, *Plasma Sources Sci. Technol.* 21, 055006 **(2012)**.
17. K. N. Kim, J. H. Lim, H. B. Jeong, G. Y. Yeom, S. H. Lee, and J. K. Lee, *Microelectronic Engineering* 89, 133 **(2012)**.
18. S. Samukawa and T. Mukai, *J. Vac. Sci. Technol. A* 17, 2463 **(1999)**.
19. H. Lee, B. S. Won, and N. E. Lee, *Thin Solid Films* 521, 83 **(2012)**.
20. A. Cruden, M. V. V. S. Rao, S. P. Sharma, and M. Meyyappan, *J. Appl. Phys.* 93, 5053 **(2003)**.

Received: 25 January 2014. Accepted: 11 April 2014.